NUMERICAL DESIGN AND ASSESSMENT OF A BIPLANE AS FUTURE SUPERSONIC TRANSPORT ------ REVISITING BUSEMANN'S BIPLANE ------

Kisa MATSUSHIMA*, Kazuhiro KUSUNOSE, Daigo MARUYAMA* and Takumi MATSUZAWA***

* Dept. Aerospace Engineering, Tohoku University, Aoba-ku, Sendai 980-8579, JAPAN.
Phone: +81-22-795-6918, Fax: +81-22-795-6979, Email: kisam@ad.mech.tohoku.ac.jp,
** Formerly Institute of Fluid Sciences, Tohoku University and
Currently Technical Research and Development Institute, Japan Defense Agency.

Keywords: *Supersonic, Aerodynamics, Busemann's Biplane, Inverse Design*

Abstract

Aiming to realize a new concept supersonic transport, aerodynamic design and performance evaluation of biplane airfoils are discussed based on Computational Fluid Dynamics (CFD). In supersonic flight, airfoils generate strong sonic booms and wave drags accompanied by shock waves. To reduce them, Busemann's biplane concept is adopted and developed.

A two-dimensional biplane configuration has been successfully designed using modern CFD simulation and a newly developed inverse problem. When the lift coefficient is more than 0.144, the designed biplane having a reasonable airfoil thickness gives lower wave drag than that of a flat plate. CFD assessment has also performed concerning the peculiar aerodynamic characteristics attributed to biplane configuration. They are hysteresis and choking phenomena which produce much amount of drag as an off-design condition. The promising strategy to avoid the drag increase is also demonstrated.

1 Introduction

The Concorde was the first but also the last commercial SST (Supersonic Transport) ever built. Its flights were terminated in 2003, due to poor fuel efficiency and unacceptable at-ground noise level. By the termination, people lost a precious choice to move around the world at supersonic speed. There will be a lot of demand for developing cost-efficient and quiet commercial supersonic airplanes. Thus, to attain low boom and low drag capability is crucial for the development of the next generation SST.

In 2004, a project of supersonic biplanes started at Tohoku University. The project has been led by one of the authors Kusunose, formerly a visiting professor of Tohoku University [1]. Its goal is to realize a quiet and energy efficient SST utilizing the Busemann's biplane concept [2,3]. Fundamental analysis as well as several trials to obtain a biplane configuration have been going on [4-8].

In this paper, the aerodynamic design of a biplane configuration using an inverse problem approach is reported in the first place. The inverse problem determines the geometry utilizing specified (target) pressure distributions. Since pressure distributions and shock wave strength along an airfoil surface can be regarded as the source of the sonic boom and drag, an inverse problem approach should be appropriate to obtain desirable biplane section airfoils. In the second place, assessment of its performance is done in wide range of flying Mach number to reveal troublesome problems and how to deal with them. Finally, a preliminary study for fuselage concept is introduced.

2 Review of Busemann's Biplane and Its Derivatives

2.1 Busemann's Biplane

It is said Busemann indicated to make thick airfoil's wave drag equal to that of flat plate by using the biplane concept at the Volta Congress in 1935[2]. Particularly, he showed how to eliminate wave drag at zero lift within the approximation of small perturbations which discarded entropy changes.

His biplane concept is to combine two airfoil elements in such a way as to promote favorable wave interactions between the two. By choosing their geometry such as half-diamond wedge shape and relative locations carefully, the waves generated by those elements would cancel each other (see Fig. 1). In Fig. 1, ε is wedge angle of Busemann's biplane and red characters, 0 and β indicate *Cp* value in the bounded domain of the space around the biplane. The *Cp* values are estimated by the supersonic linear theory. Accordingly, along the upper surface of the upper element and the lower surface of the lower element, *Cp* is zero everywhere. On the other hand *Cp* along the lower surface of the upper element and the upper surface of the lower element is β. No pressure-wave disturbances appear outside of the biplane. This proposal encouraged many researchers and they published interesting articles[9-12]. Wolcher considered nonlinearity of wave interaction and propagation and tried to obtain desirable shapes[9]. Ferri conducted wind tunnel experiments around Mach number of 2.0 and found hysteresis phenomena[10]. However, Busamann's paper regarding sonic booms in 1955 [13] might have discouraged researchers from working on the biplane. In the 1955 paper, he disclosed that the biplane was not almighty especially for the sonic boom due

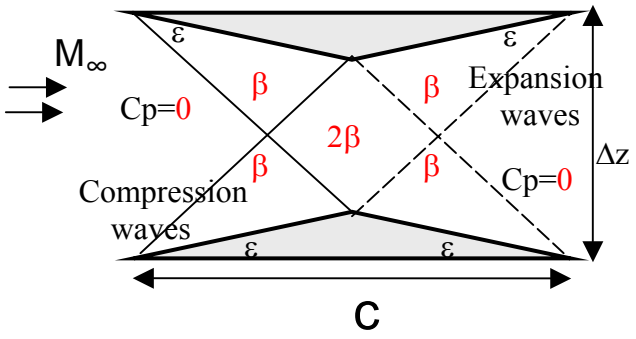

Fig. 1. Busemann's Biplane and Its Physics.

to lift. He concluded the paper with the following words; 'the sonic boom problem is severe, but also the laws of nature are not systematically ganging up to prevent any solution.' The authors would believe in that some solution could exist.

2.2 Licher Type Biplane

One of the most interesting derivatives from Busemann's biplane was proposed by Licher in 1955[14]. This particular biplane configuration exhibits that the wave drag due to lift can be reduced to 2/3 of that of a single flat plate under

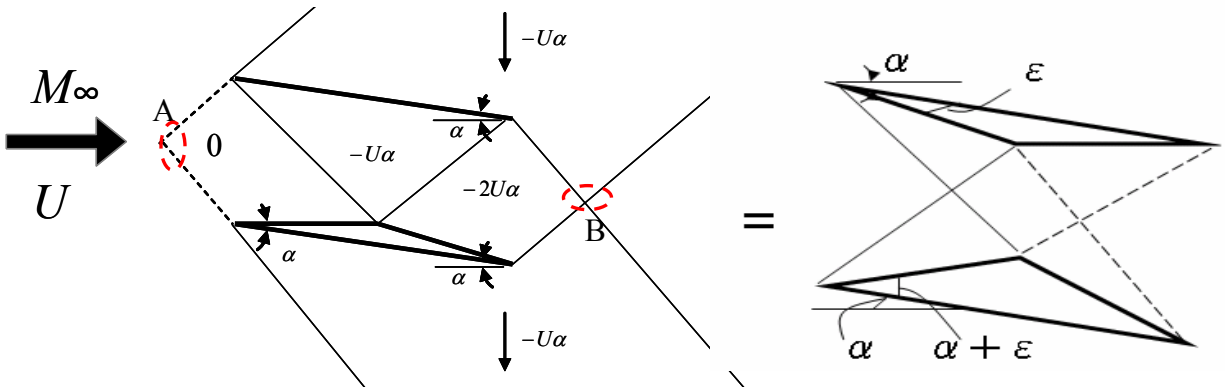

Fig. 2. Licher Type Biplane : Aerodynamic Model (left) and Realistic Biplane (right)

the same lift condition by utilizing favorable wave reflections on internal surface of the upper and lower elements. The aerodynamic model in Fig. 2 (left side one) explains the drag reduction mechanism. The chord lengths of both the upper flat plate and lower half diamond airfoil are assumed C. The special combination of them produces the same pressure wave disturbance spreading in the space as that of the flat plate whose chord length is 1.5C. It is well known that to distribute load on a longer distance lowers drag. In order to obtain a Licher type biplane, a Busemann type biplane is added to the aerodynamic model of Fig. 2. Then, one obtains the new lifted biplane system having the angle of attack of α degrees. The lower element is thicker than the upper. We think it causes the same effect as camber for a single airfoil.

2.3 CFD Analysis of Both Biplanes

To evaluate aerodynamic performance, we conducted Euler simulation using TAS (Tohoku University Aerodynamic Simulation) GRID and TAS FLOW [15]. TAS GRID is unstructured mesh generation software while TAS FLOW is a Navier-Stokes/Euler flow solver. Both are in-house software. TAS abbreviates Tohoku University Aerodynamic Simulation.

We set the flight Mach number at 1.7 as our first modern investigation of those biplanes proposed more than a half century ago. For the Mach number of 1.7, an arranged Busemann's biplane has 5.7 degrees as ε and 0.5C as Δz in Fig.1 and a Licher type one has the same ε and Δz and 1 degree as α shown in Fig.2. Each element of both biplanes has at least 5%-chord thickness which sum up to at least 10% as the total t/c.

Results of the CFD analysis of both biplanes are summarized in Fig. 3 as drag polar curves. The curve of a flat plate (no thickness) are also plotted there for reference. Comparing with the data of 10% t/c diamond airfoil which showed

the *Cd* of 0.0289 at zero lift and *Cd* of 0.326 at *Cl*=0.10, we can confirm biplanes' advantage in wave drag reduction. In addition, the Licher type biplane reduces wave drag due to lift to 2/3 for lifted cases.

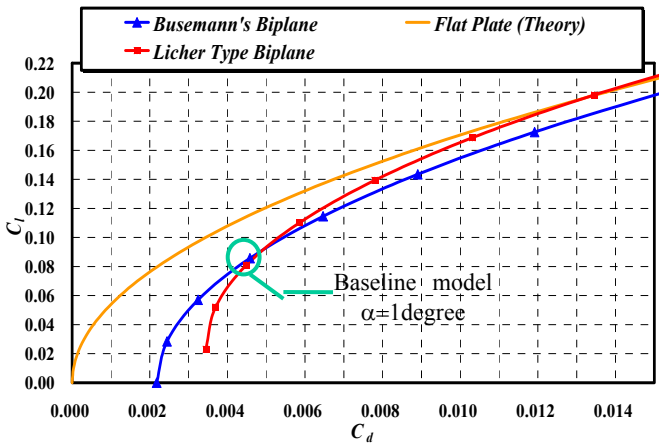

Fig.3. Aerodynamic Performance of Biplanes Predicted by Euler Simulation.

3 Creating New Biplane Geometries by CFD Inverse Problem Method [16]

3.1 Design Condition

The present design was to obtain airfoil geometry that realizes better performance than afore-mentioned two biplanes. The design Mach number was 1.7. As shown later, our design method requires initial (baseline) model as well as target pressure distributions which imply design concept. We chose the Licher type biplane as an initial model and the design point is at 1.0 degree angle of attack. It is circled in Fig. 3. Figure 4 shows target *Cp* distributions with red lines as well as the surface *Cp* distribution of the baseline with blue lines. Our design concept is as follows; 1. To have its biplane upper element generate more lift at the upper surface; 2. To have the biplane upper element generate more lift and thrust at the lower surface of the upper element near the trailing edge; 3. To make pressure waves interaction more desirable at the mid-chord apex.

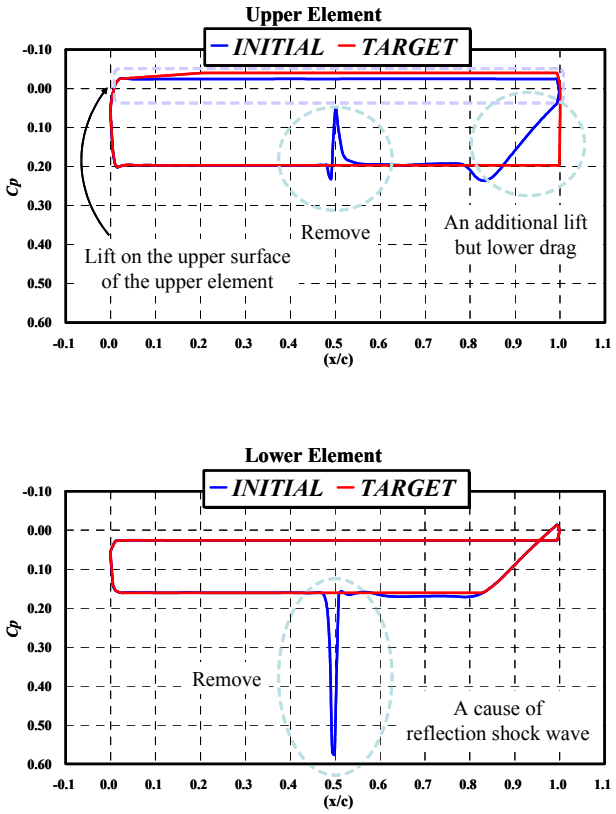

Fig. 4. Target and Initial Cp Distributions of Each Element

3.2 Design Procedure

Figure 5 illustrates the iterative procedure of the method. First, the flow field around a baseline configuration is analyzed to obtain initial *Cp* distribution of the airfoil. Next the inverse problem is solved to calculate geometry correction Δf utilizing the pressure difference between the target and the currently realized Cps. The airfoil geometry is updated by integrating the geometry corrections; We, then, go back to flow-field analysis of the updated airfoil. By repeating these procedures (a design loop), a desired airfoil will be obtained. For the present design, a Licher type biplane was adopted as the initial configuration. There are two wing elements in the biplane, so the two section airfoils of the upper and lower planes are designed. Since they strongly interact with each other, simultaneously special care has been taken in the design loop shown in Fig. 5 has been customized to be able to precisely evaluate

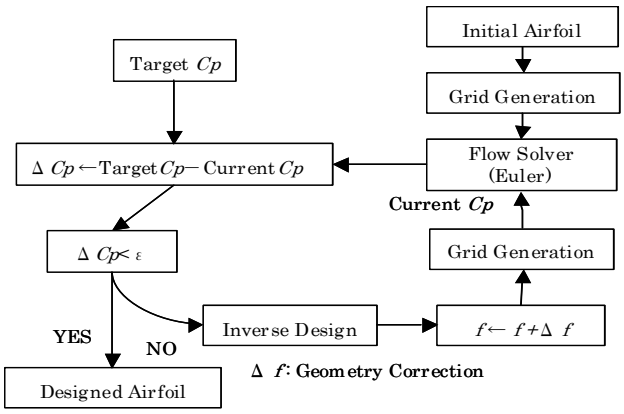

Fig. 5. Design System using Inverse Problem and CFD simulation

the change of interacting effect by the geometry change.

3.3 Basic Equation for Inverse Problem

The design method determines airfoil geometry is based on the equation of the local oblique shock relation[2,3];

$$Cp = c_1\theta + c_2\theta^2 \qquad (1)$$

where

$$c_1 = \frac{2}{\sqrt{M_\infty{}^2 - 1}}, \qquad c_2 = \frac{(M_\infty{}^2 - 2)^2 + \gamma M_\infty{}^4}{2(M_\infty{}^2 - 1)^2}.$$

θ represents the local flow deflection angle. c_1 and c_2 are called the Busemann coefficients. In the sense of airfoil geometry, θ is interpreted as $\theta = \left(\frac{\mathrm{d}f(x)}{\mathrm{d}x} - \alpha\right)$, where $f(x)$ is an airfoil contour curve, x is the chord direction and α is the angle of attack. The design method in Fig. 5 counts the non-isentropic physics because Euler/Navier-Stokes flow calculation is adopted in the design loop.

3.4 Design Process and Results

After fourteen iterations of the loop, the design converged. In Fig. 6, surface *Cp* distributions realized by the designed biplane elements are plotted in comparison with the target pressure distributions. The red lines are

the *Cp* distribution around the designed and the blue lines indicate the corresponding target *Cp*. Agreement of the target and realized *Cp* distributions is very well. Observing the designed shape in detail, the trailing edge of upper element of the designed biplane configuration was getting thinner. The lower surface of the upper element had a concave curve parallel to the outer flow direction along the upper surface. The compression waves generated at the leading edge of both elements and a part of the expansion waves generated at the mid-chord apex of the elements cancelled each other, eliminating the pressure peaks at the mid-chord throat. The rest of the expansion waves cancelled out with the compression wave generated by the concave curve in the vicinity of the trailing edge.

Then, the parametric Euler analysis with varying the flight angle of attack was conducted using the TAS code. Consequently, at the design point, the designed configuration had more lift to drag ratio (*Cl*=0.1154, *Cd*=0.00531, L/D=22) than the initial one (a Licher type biplane) which had *Cl*=0.0812, *Cd*=0.00449, and L/D=18.

The results are summarized in Fig. 8, which compares the drag polar plot of the designed biplane with that of the Licher type baseline, original Busemann's biplane and the flat plate. Over a range of sufficient lift (0.1<*Cl*<0.2), the designed biplane realized *Cd* reduction by 10 to 15 counts (1 count = 0.0001), compared to the Licher type baseline model.

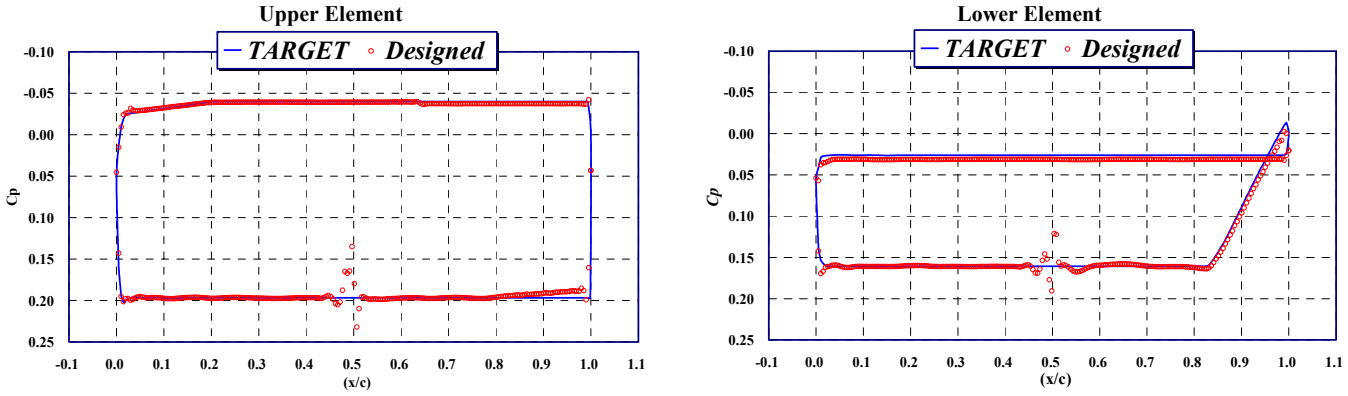

Fig. 6. Cp Distributions of Designed Elements of Biplane (red symbols) and Target Cp

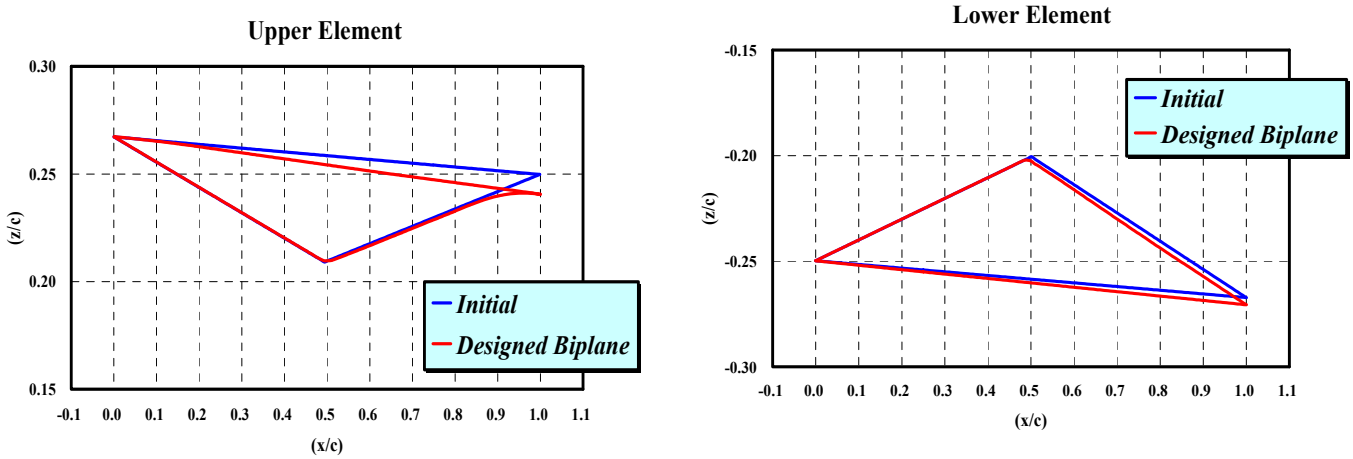

Fig. 7. Geometries of the Upper and Lower Elements of Designed Biplane Compared with Those of the Initial Baseline.

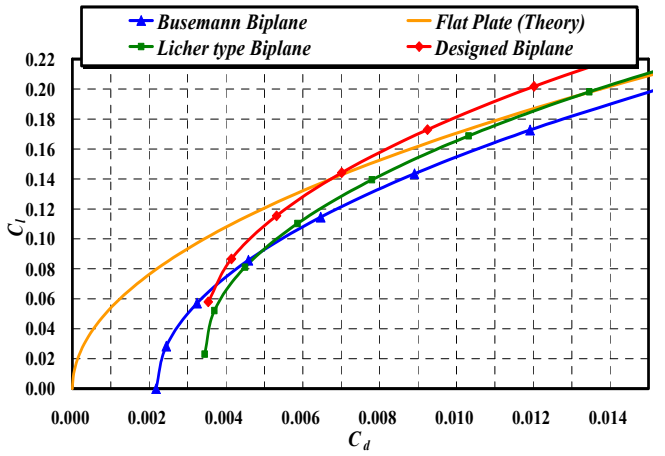

Fig. 8. Aerodynamic Performance of Designed Biplane Predicted by Euler Simulation Compared with Original Biplane Models.

4 Aerodynamic Assessment for Phenomena Peculiar to Biplanes

In this section, phenomena that are inherent to a biplane are discussed. Since the geometrical configuration is rather similar to an engine intake than a single airfoil (mono-plane), the traditional supersonic wing knowledge might not be very useful for a biplane. So, assessment is needed. The assessment was done by CFD using TAS software system. As the model of a biplane, the arranged Busemann's in Section 2.3 was used.

4.1 *Cd* Characteristics in Flight Mach Number Range

Figure. 9 shows wave-drag variation over a range of flight Mach numbers ($0.3 \le M_\infty \le 3.0$), including the would-be cruise Mach number 1.7. It is a good news that we can observe a range of Mach numbers ($1.65 \le M_\infty \le 2.0$) where wave drag remains nearly its minimum value. The existence of this low wave-drag range is positively critical for the development of real life SST in the future. However, there exists a high wave-drag range of Mach numbers where wave drag is even higher than that of the diamond airfoil of the same volume. High wave drag is caused by a strong bow shock formation

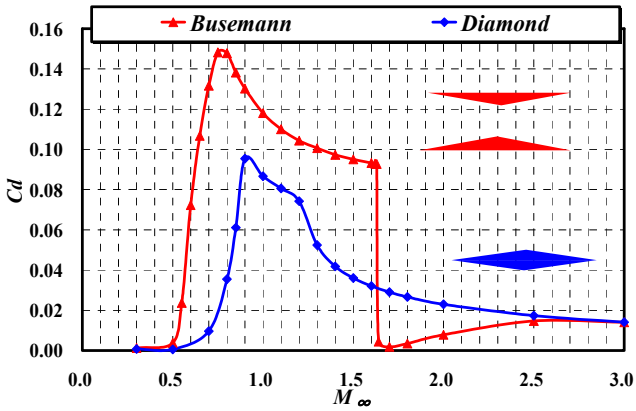

Fig. 9. *Cd* Characteristics of Biplane and Diamond Airfoil

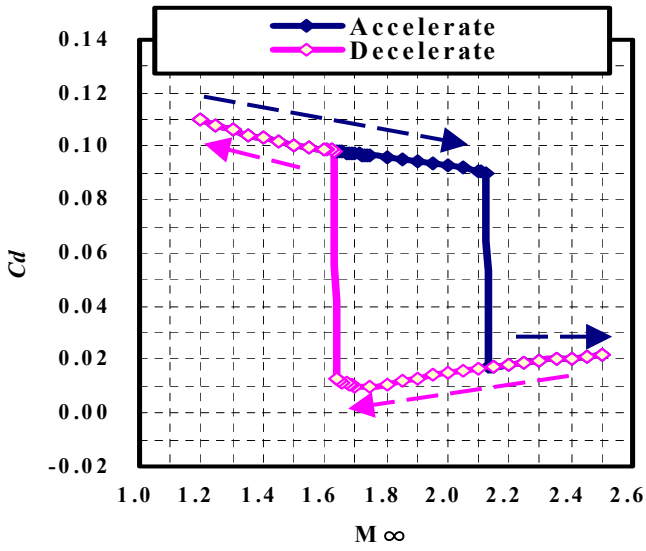

Fig. 10. *Cd*- M_∞ Hysteresis of Biplane.

upstream of a biplane. Studies are required to overcome the penalties of high-drag in $0.6 \leq M_\infty \leq 1.64$ to let supersonic biplanes to be fuel-efficient.

4.2 Hysteresis

In real flight, an airplane accelerates from taking off to cruising and decelerates when landing. Then, it is necessary to simulate the chronological process of acceleration and deceleration which might cause unsteady and hysteresis phenomena. In Fig. 10, the results of the chronological simulation are summarized in terms of *Cd* and flight Mach numbers. It was detected that hysteresis occurred at the flight speed ranging $1.65 \leq M_\infty \leq 2.12$. This result well agreed with the one-dimensional theory of starting and unstarting condition for an intake diffuser. This disadvantage can be resolved by inlet area section control (see **4.3**) using evolved Busemann's biplane in Fig. 11.

The acceleration and deceleration processes were visualized as *Cp* contour maps shown in Fig. 12. Each color represents a *CP* value. Corresponding *Cp* values decrease in the order of red, yellow, green, light-blue(*Cp=0*) and dark-blue. We observed that detached shock waves were generated at an upstream location of the biplane and they got closer to the leading edge as the flight Mach number increased. Then, on a certain Mach number, the shock waves were swallowed and moved to a downstream location of the throat. Therefore chocking disappeared. This corresponds to that of starting process of intake diffuser.

4.3 Control of Inlet Section Area

To overcome the high drag choking on the acceleration process due to hysteresis, we expected the inlet area control was useful because the phenomena were described by the one dimensional equation. According to the equation, the essential parameter is the ratio of *A2/A1* shown in the following figure. *A1* and *A2* are the section areas of inlet and the throat, respectively. Thus, the control was done by hinged leading edge devices.

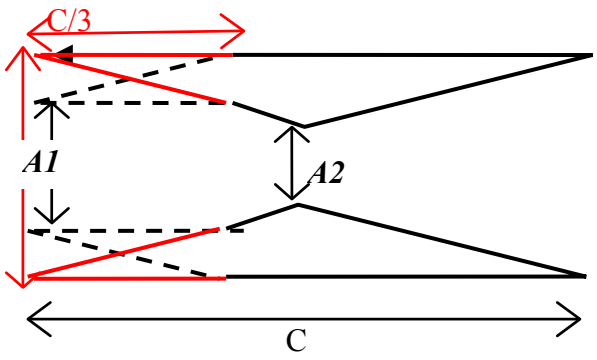

Fig. 11. Busemann's Biplane with Control Devices

The Navier-Stokes simulations of Busemann's biplane were done at the point of M_∞=1.7 in the acceleration process. It started with the ratio of 0.8, which yielded to the *Cd* of about 0.1. Then, we continued the simulation increasing the ratio.

As seen in Fig. 13, when the ratio reached to 0.88, the *Cd* value catastrophically dropped because the detached shock waves disappeared. Once that happened, we could set the ratio at the arranged value of 0.8 and realized the lowest *Cd*.

The same kind of control can be used to suppress high-drag choke situation mentioned in Section **4.1** [7,8].

5 Fuselage Concept [17]

We are now conducting a fundamental study for fuselage. The essential concept for fuselage design is to eliminate the source of sonic boom. One of the authors, Kusunose has proposed the aerodynamic model of fuselage, which has a flat bottom. The simplified models in the two and three dimension are shown in Fig.14. The idea is that pressure-wave disturbance toward the ground would be eliminated in non-lifting cases and reduced otherwise when the bottom line/plane is parallel to the air flow stream direction. The results of the study will be presented at the conference in September.

6 Conclusions

Aiming to realize low boom and low drag SST, a biplane airfoil configuration was designed and

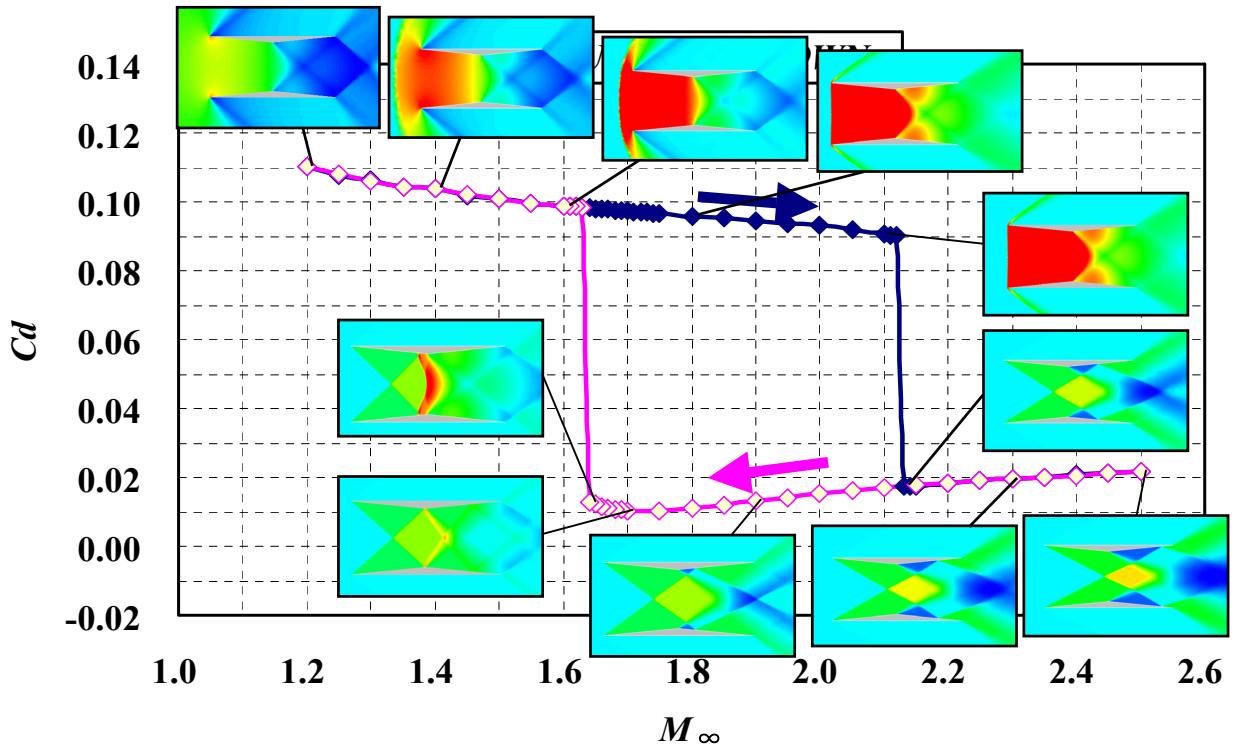

Fig. 12. Visualization of Hysteresis Process with *Cp* Contour Maps.

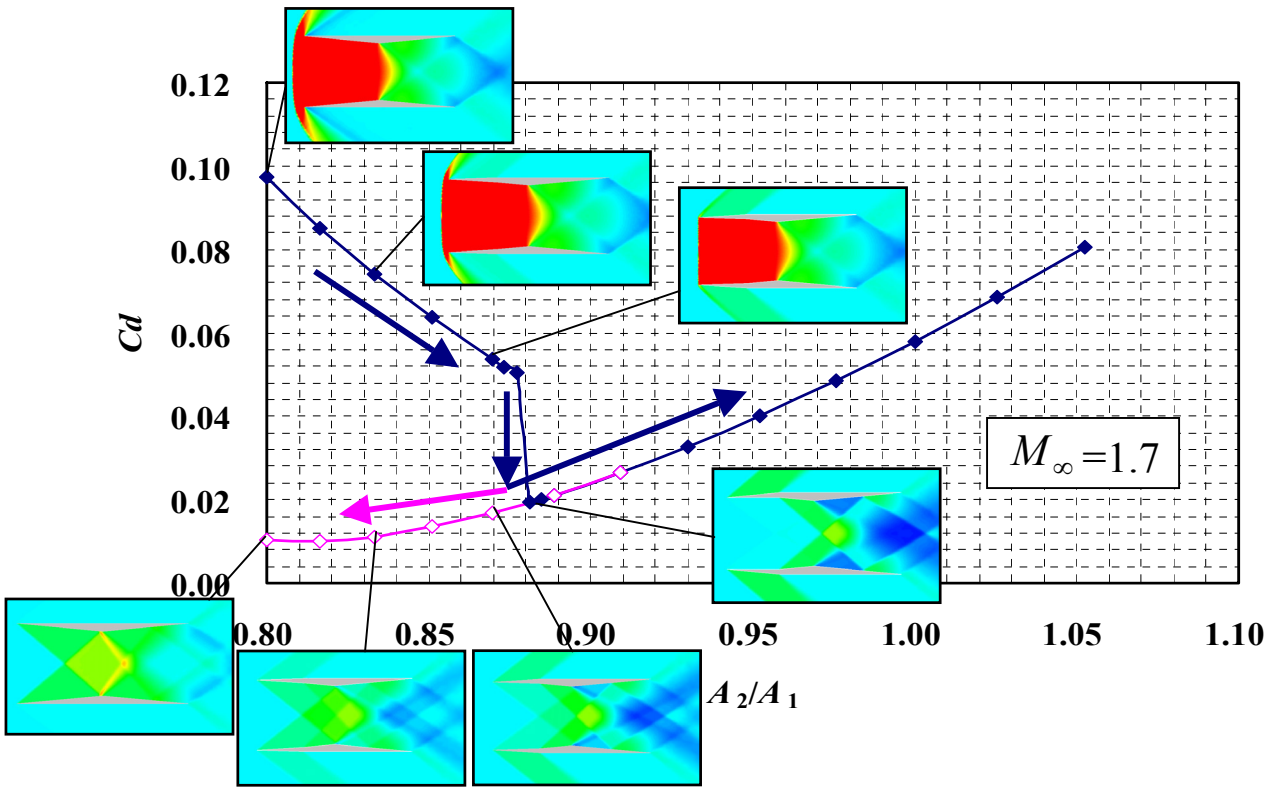

Fig. 13. Inlet Area Control to Avoid Choking and Visualization with *Cp* Contour Maps.

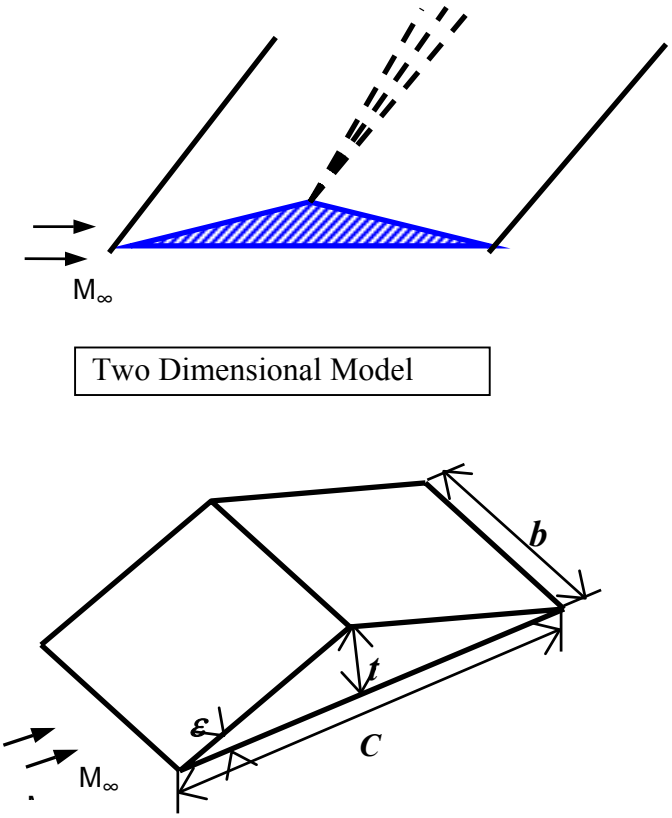

Fig. 14. Concept Overview for Low-boom Fuselage [17].

analyzed. First, we revisited Busemann's biplane and confirmed the advantage of a biplane configuration in terms of wave drag reduction capability.

Then, new biplane section airfoils have been designed by the inverse problem approach. The designed configuration has shown good performance. Especially when Cl>0.14, wave drag is less than that of a single flat plate airfoil. It is notable that a biplane configuration had a sufficient thickness ($t / c \cong 0.10$), while a flat plate has no thickness.

Next, the assessment of the inherent aerodynamic characteristics in a biplane was done by modern CFD. It was observed that chocking occurred over a wide range of free stream Mach numbers, from 0.5 to 1.64. Moreover, simulations were run to estimate the acceleration path up to the Mach number of 2.6. The results confirmed the hysteresis of un-starting and starting situations. And they were found in agreement with the theory of one-dimensional flow of intake diffusers. After careful analysis and consideration, by the ratio control of the inlet section areas to the throat one, hysteresis was effectively avoided as well as wave drag was significantly reduced.

Finally, the ongoing study for low-boom fuselage design was introduced. We believe utilizing the above-mentioned biplane concepts will enable fuel-efficient and quiet SST to be realized.

7 Acknowledgments

We would like to thank Professor K. Nakahashi, Professor S. Obayashi of Tohoku University and Professor A. Sasoh of Nagoya University for many valuable discussions and comments over the course of developing the present research.

8 References

[1] Kusunose, K. A New Concept in the Development of Boomless Supersonic Transport, Proc. First International Conference on Flow Dynamics, Sendai, Japan, November 2004.

[2] Busemann, A. Aerodynamic lift at Supersonic Speeds, Luftfahrtforschung, Ed.12, Nr.6, Oct.3, 1935, pp.210-220.

[3] Liepmann, H. W. and Roshko, A., Elements of Gas Dynamics, John Wiley & Sons, Inc., New York, 1957.

[4] Maruyama, D., Matsushima, K., Nakahashi, K., and Kusunose, K. Aerodynamic Design of Low Boom and Low Drag Supersonic Biplane, Proc. Second International Conference on Flow Dynamics, OS7-2, November 2005.

[5] Yenezawa M.,Yamashita H., Goto Y., Kusunos K and Obayashi S. Wing Tip Effect of Busemann's Biplane, Proc. Second International Conference on Flow Dynamics, OS7-3, November 2005.

[6] Yamashita H., Yenezawa M., Goto Y., Obayashi S. and Kusunos K. CFD Analysis of Shock Wave for Busemann's Biplane, Proc. Second International Conference on Flow Dynamics, OS7-4, November 2005.

[7] Kusunose K., Matsushima K., Goto Y., Yamashita H., Yonezawa, Maruyama D. and Nakano T. A Fundamental Study for the Development of Boomless Supersonic Transport Aircraft, the 44th

AIAA Aerospace Sciences Meeting and Exhibit, AIAA paper 2006-0654, January 2006.

[8] Maruyama, D., Matsushima K., Kusunose, K. and Nakahashi, K. Aerodynamic Design of Biplane Airfoils for Low Wave Drag Supersonic Flight, the 24th Applied Aerodynamics Conference, AIAA 2006-3323, June 2006.

[9] Walcher V. O. Discussion on aerodynamic drag of wings at supersonic speed using biplane concept, Luftfahrtforshung, 14, pp. 55-62, 1937.

[10] Ferri A. Experiments at supersonic speed on a biplane of the Busemann type, British R.T.P Trans. No.,1407, 1944.

[11] Moeckel W.E Theoretical aerodynamic coefficients of two-dimensional supersonic biplane, NACA T.N. No.1316, 1947.

[12] Lighthill, M. J. A Note on Supersonic Biplane, British A.R.C. R.&M. No.2002, 1944.

[13] Busemann A. The relation between minimized drag and noise at supersonic speed, Proc. Conference on High-Speed Aeronautics. Poly. Inst. Brooklyn, Jan.20-22, pp. 133-144. 1955.

[14] Licher R. M. Optimum Two-dimensional Multiplanes in Supersonic Flow, Report S. M. 18688, Douglas Aircraft Co., 1955.

[15] Nakahashi, K. Ito, Y., and Togashi, F Some Challenge of Realistic Flow Simulations by Unstructured Grid CFD, Int. J. Numerical Methods in Fluids, Vol. 43, pp.769-783 2003.

[16] Matsushima, K. Maruyama, D., Nakano, T., and Nakahashi, K. Aerodynamic Design of Low Boom and Low Drag Supersonic Transport using Favorable Wave Interference, Proc. The 36th JSASS Annual Meeting, April, 2005, pp. 130-133, 2005.

[17] Kusunose. K, What is the fuselage geometry of SST which generates no strong shock waves?, to be presented at the third S3T Meeting in June 22, 2006, Aerodynamics Division of JSASS, 2006.